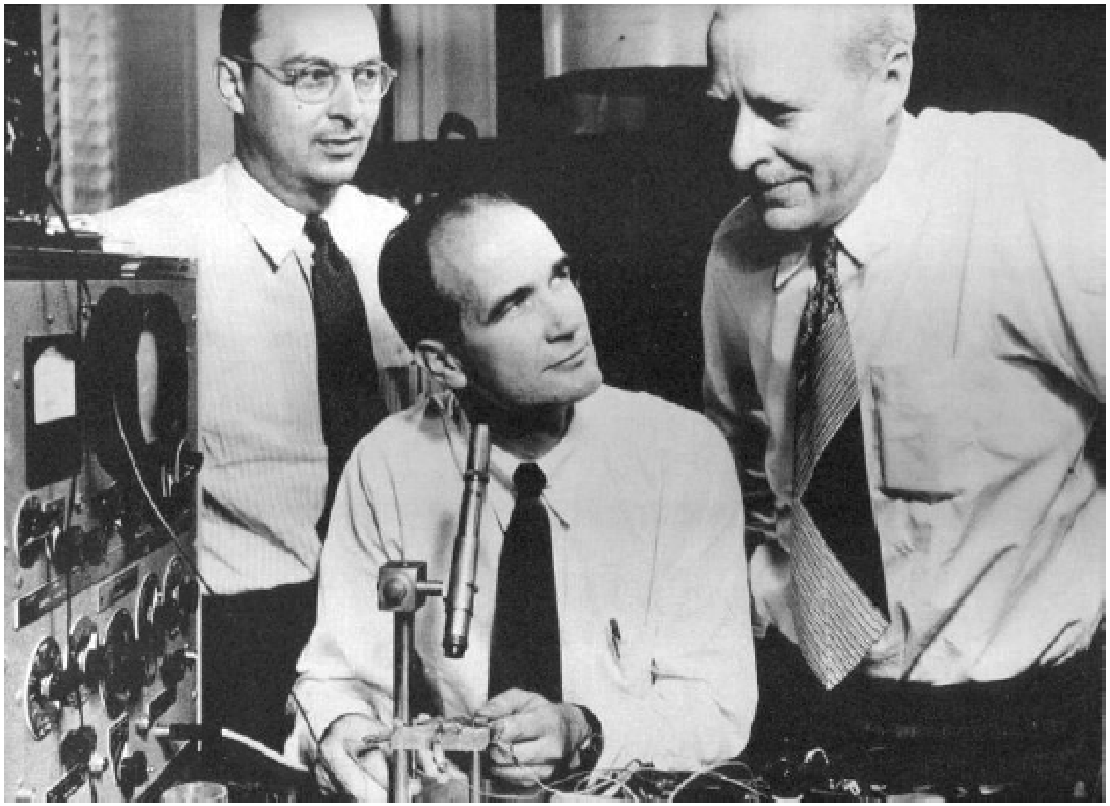

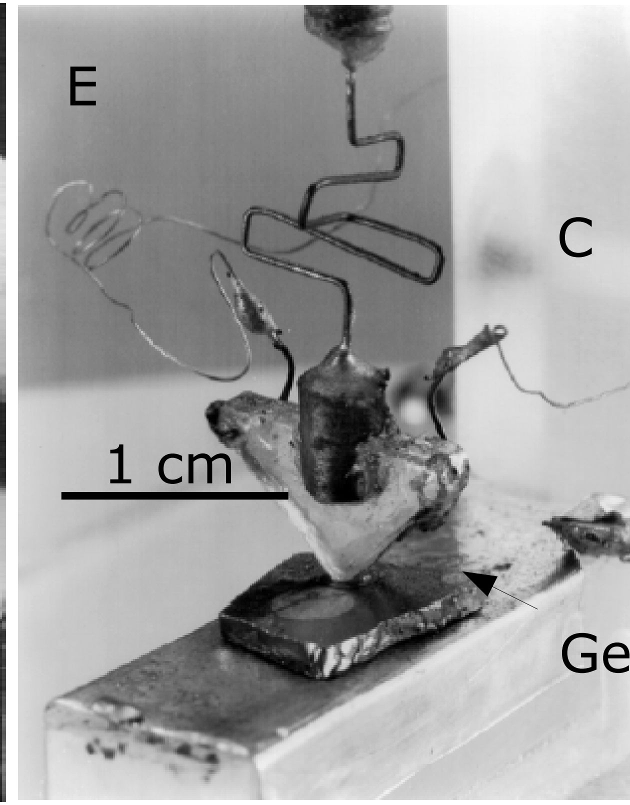

John Bardeen**, William B. Shockley und Walter Brattain (v.l.n.r., 1956) erfanden den bipolaren Transistor 1947 in den Bell Laboratories

Originalversuchsaufbau (Quelle: Lucent Technologies)

pnp-Transistorverstärkerschaltung

kleine Änderung i_B des Basisstroms I_B

$\rightarrow$ große Änderung i_c des Kollektorstroms I_c

(oder: kleines u_{ein} $\rightarrow$ großes U_{Rv})

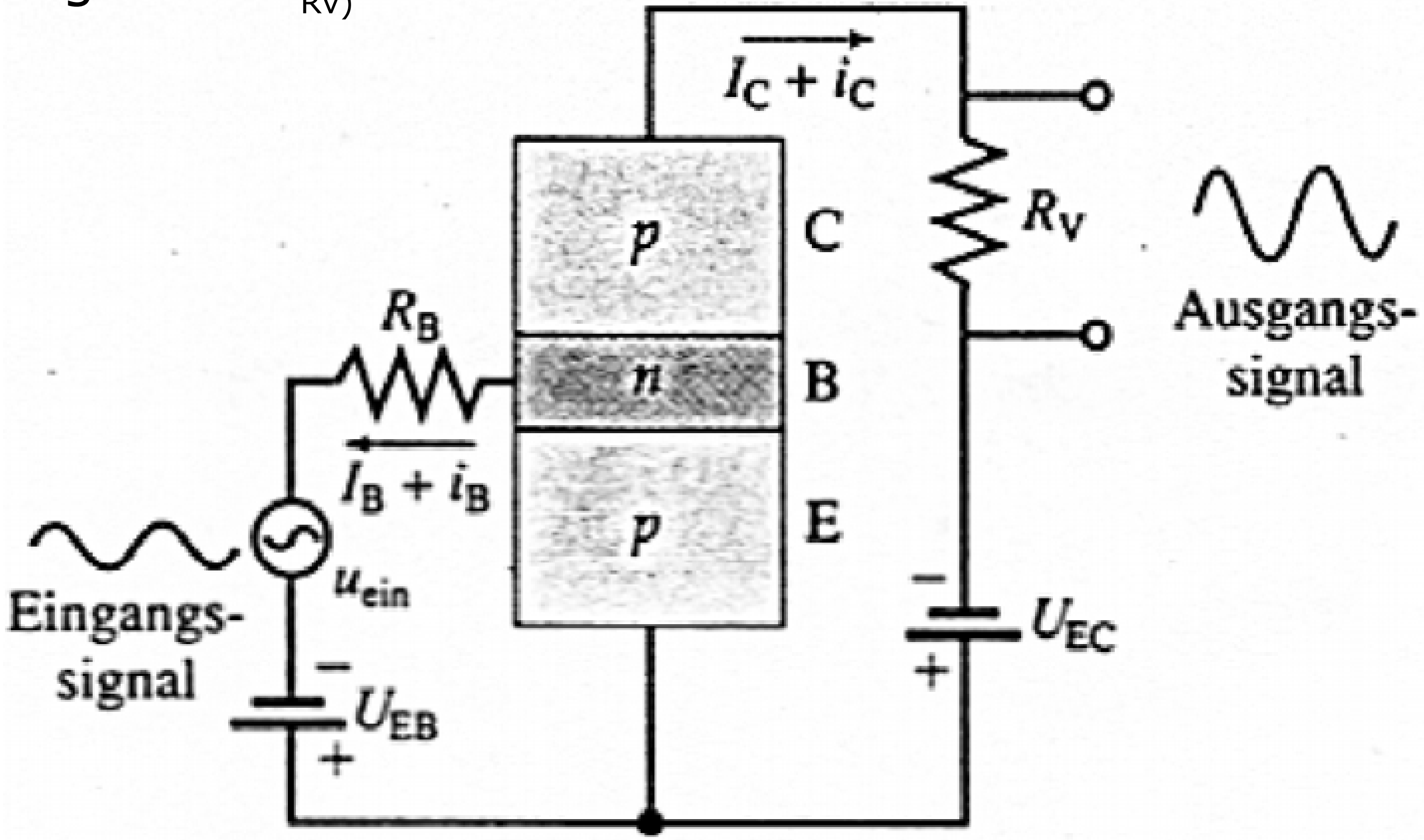

npn-Transistor

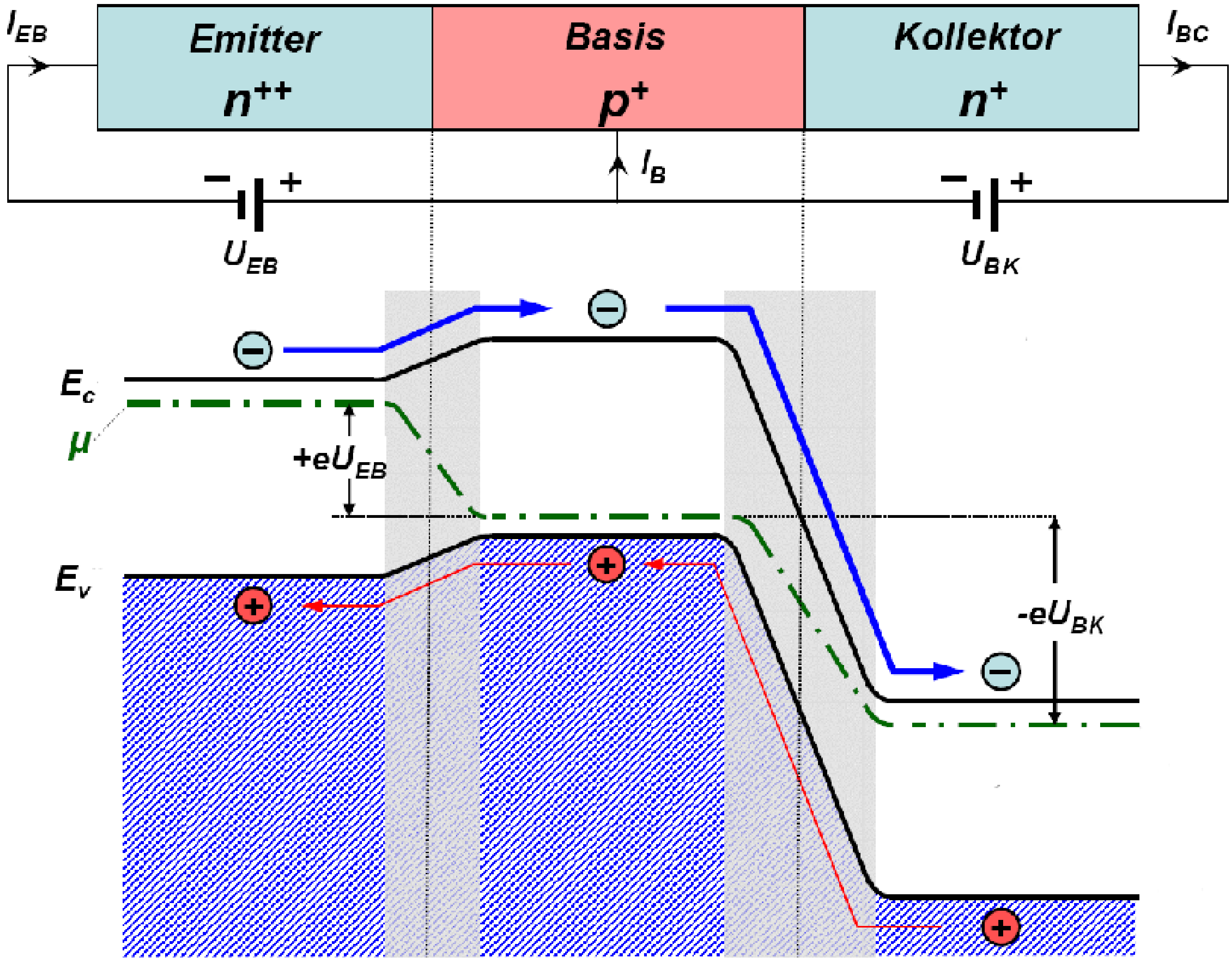

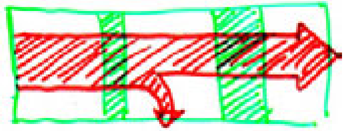

EB in Durchlass-, BK in Sperrrichtung; Basis dünn gegen Diffusionslänge; über EB injizierte Ladungsträger diffundieren (transistor!) zu K; dort durch Sperrspannung abgesaugt

n.b.: dicke Basis hat Strom 0 zur Folge

MOSFET

Metal-Oxide-Semiconductor Field Effect Transistor (1960)
Julius E. Lilienfeld, U.S. Patent 1, 745, 175 (1930)
Oskar Heil, British Patent 439, 457 (1935)

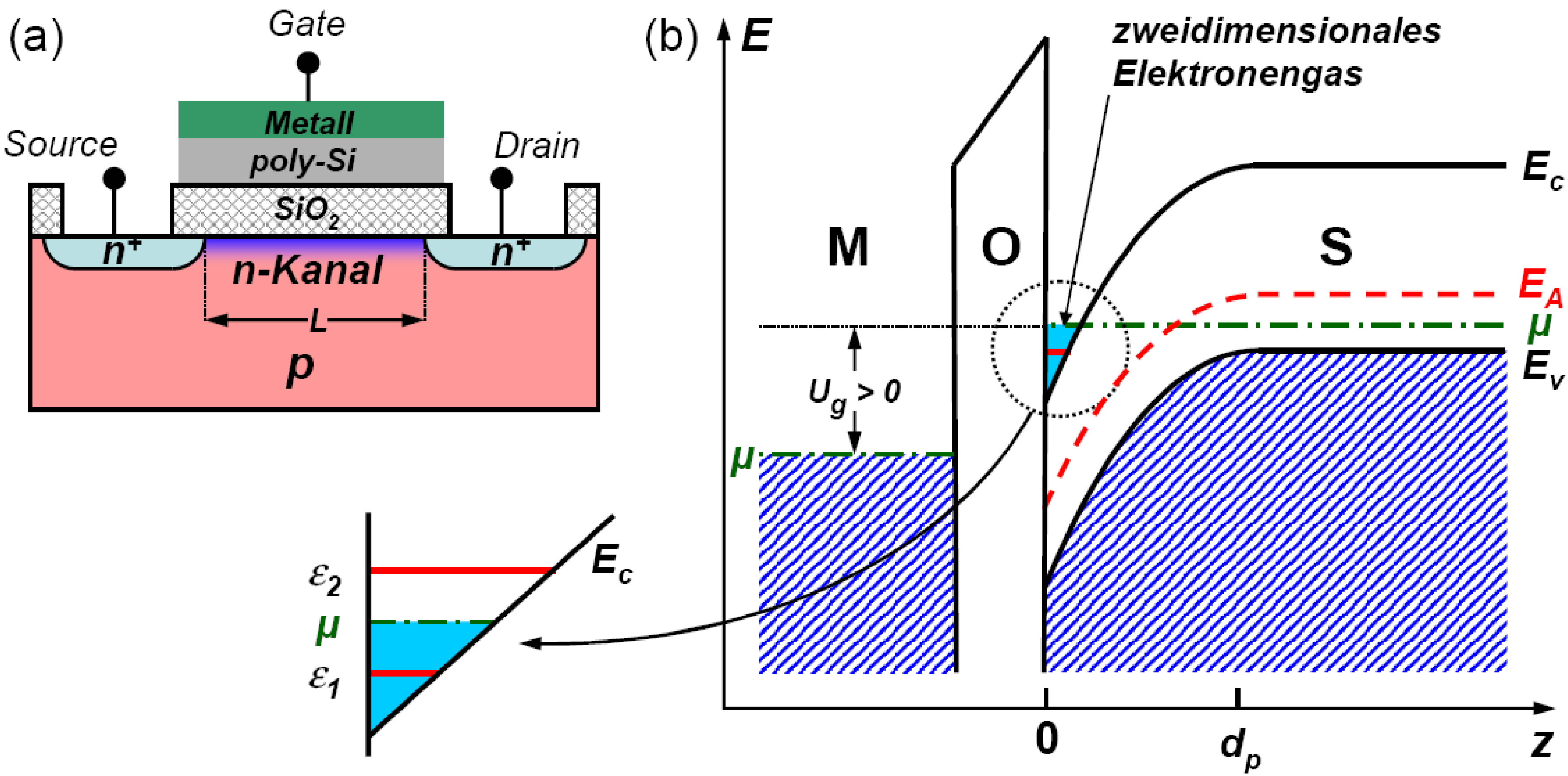

MOSFET Gate-Spannung Ug > 0

Gate-Feld hält Elektronen im Kanal

Dreieckspotenzial an Grenzfläche p-Halbleiter/Oxidschicht: 2DEG

hier unterstes Subband besetzt

"Nebeneffekt":

Niedrigdimensionale Elektronensysteme

Quantentrog (quantum well)

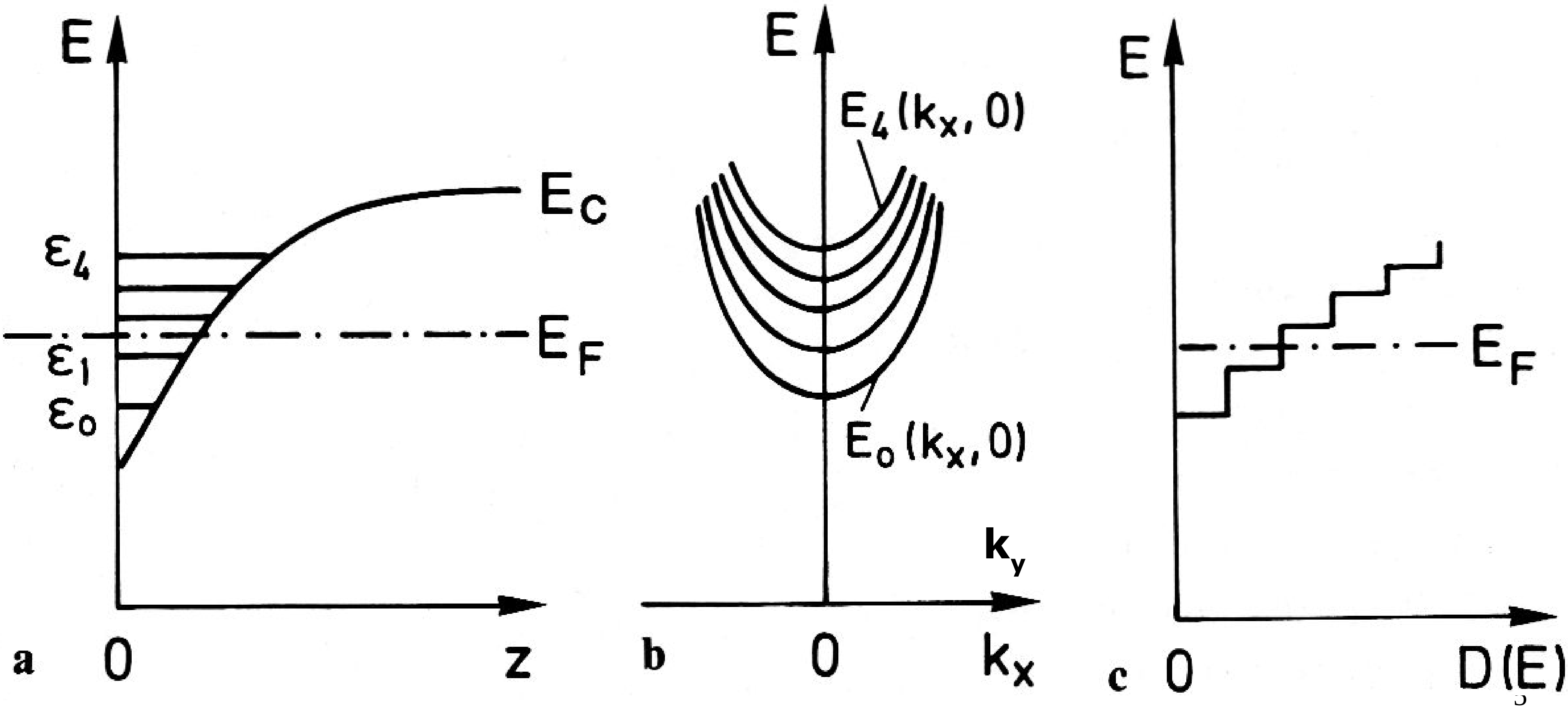

Andere Realisierung: Heterostrukturen

Binäre Verbindungen: GaAs

2- oder Mehrlagensysteme

Ternäre Verbindungen: $Al_xGa_{1-x}As$

Quaternäre Verbindungen: $Ga_xIn_{1-x}As_yP_{1-y}$

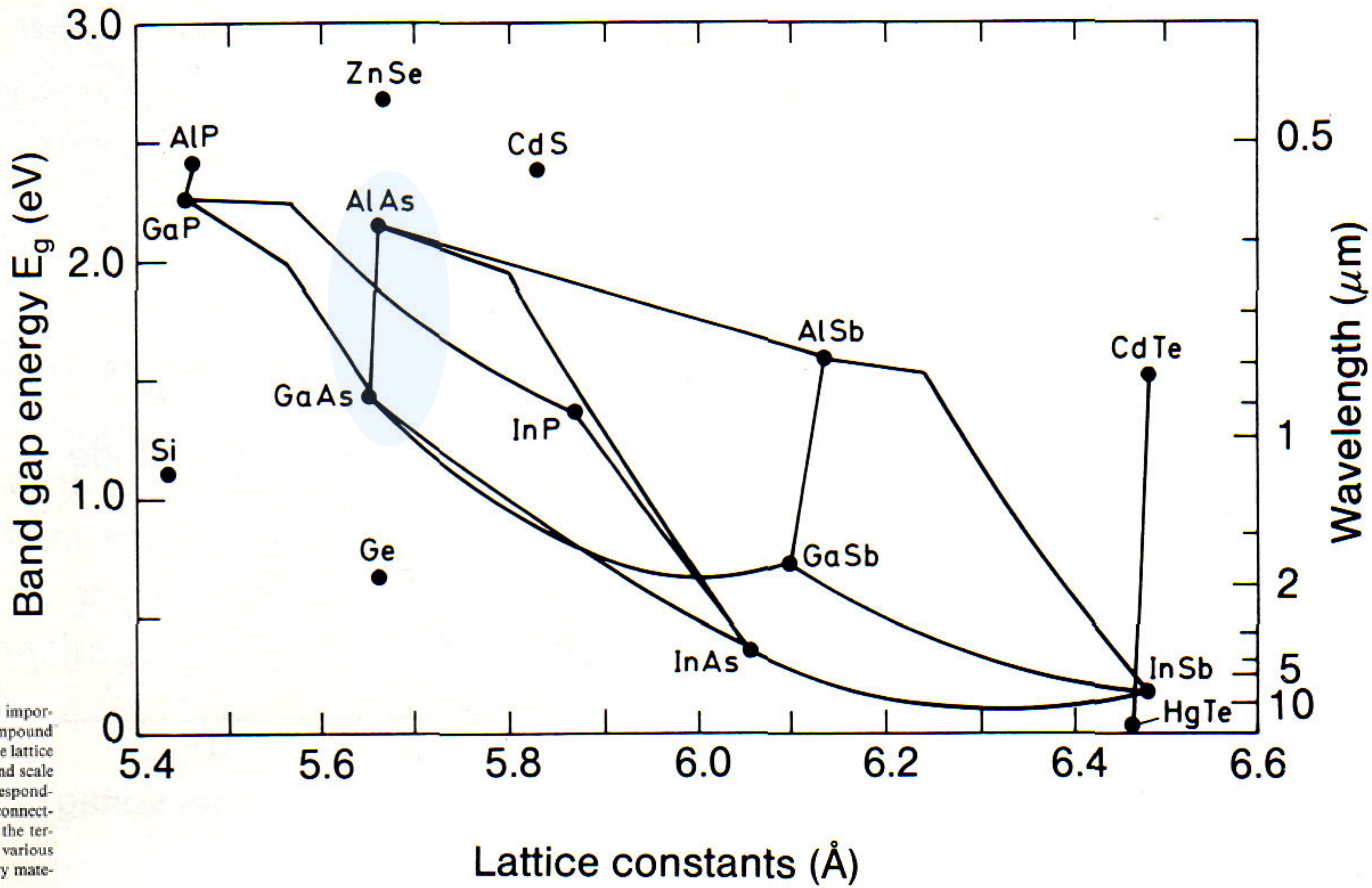

Fig. 12.21. Band gap E_g of some important elemental and binary compound semiconductors plotted against the lattice parameter at 300 K. The right-hand scale gives the light wavelength λ corresponding to the band gap energy. The connecting lines give the energy gaps of the ternary compounds composed of various ratios of the corresponding binary materials

Molekularstrahlepitaxie (MBE)

Metal Organic Chemical Vapour Deposition (MOCVD)

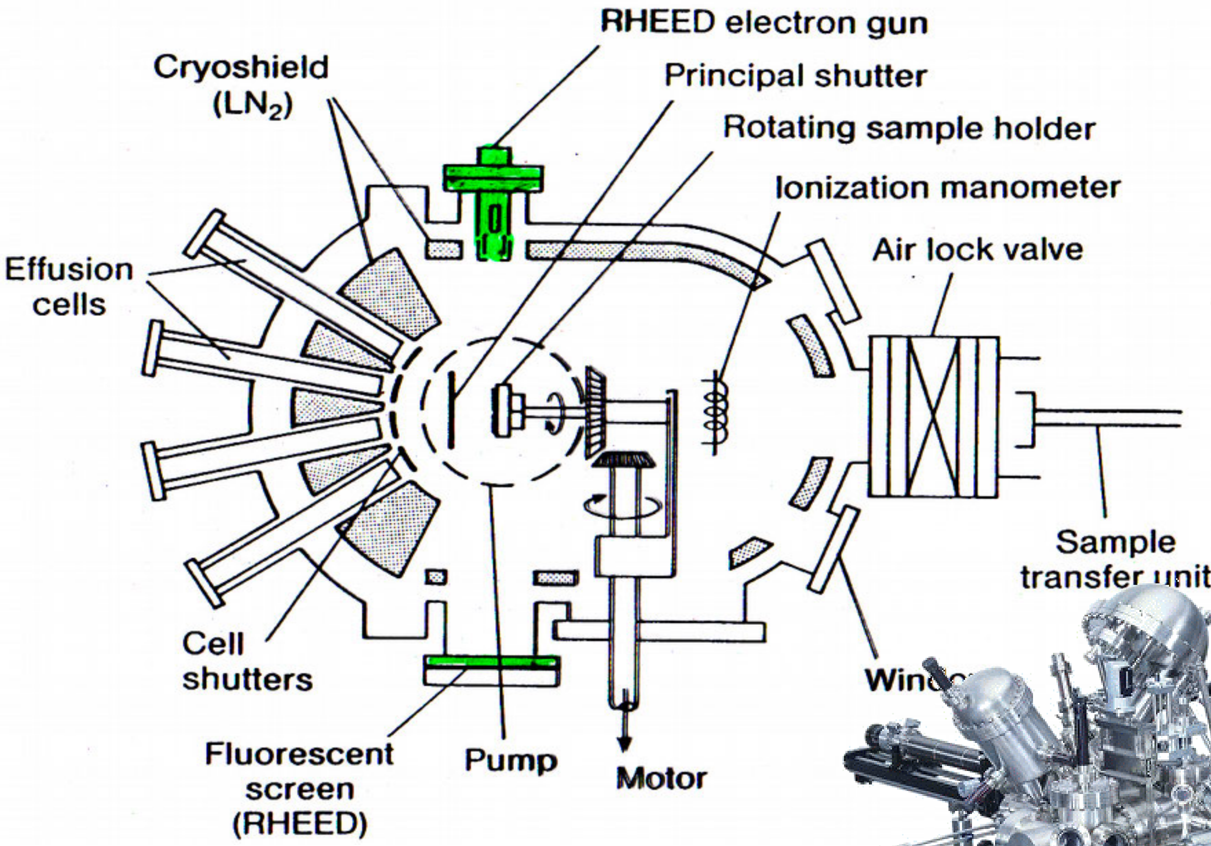

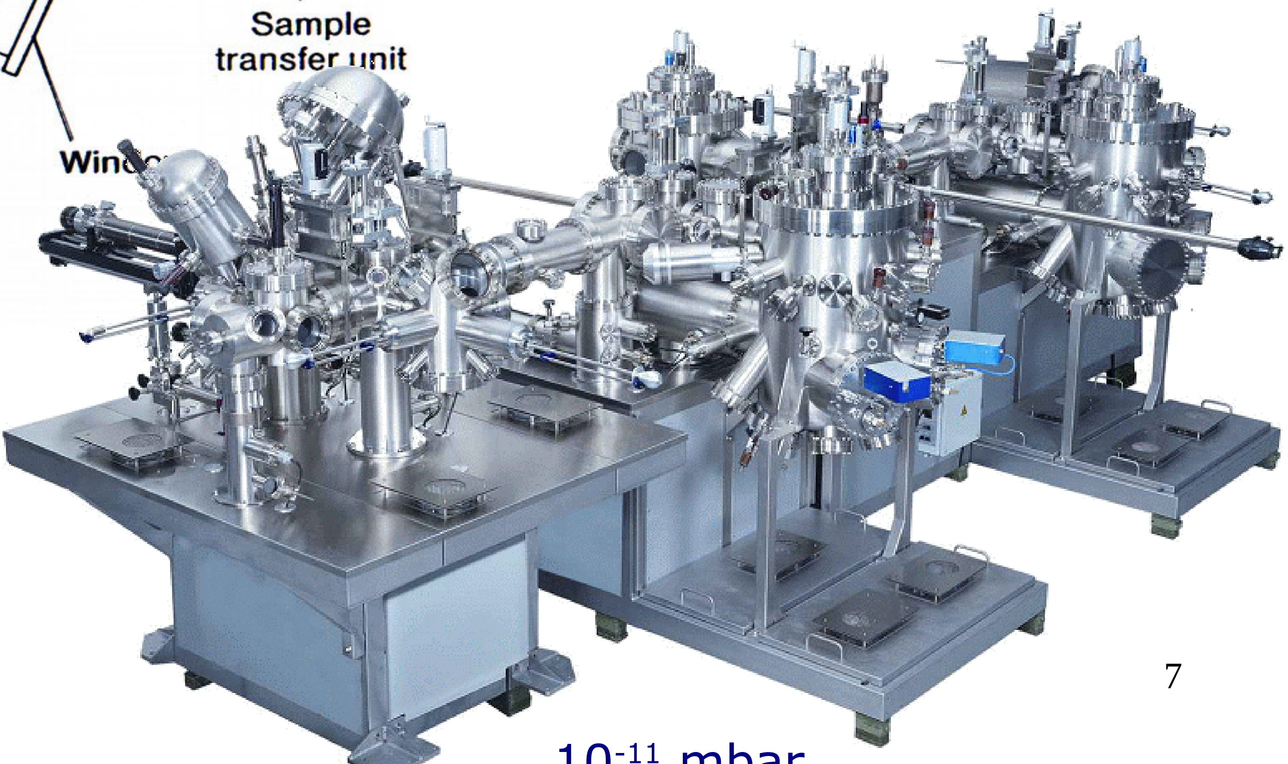

10^{-11} mbar

Ausdehnung der Übergangszone ?

Strukturell: 1 Atomlage

Elektronisch:

Bandlücke 1 Atomlage

Bandverbiegung λ_D (≈10 nm)

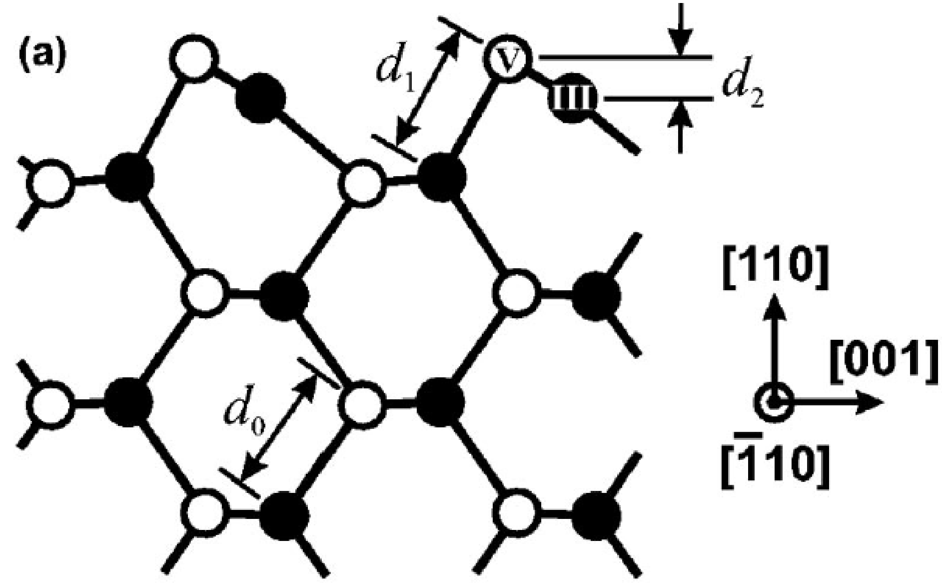

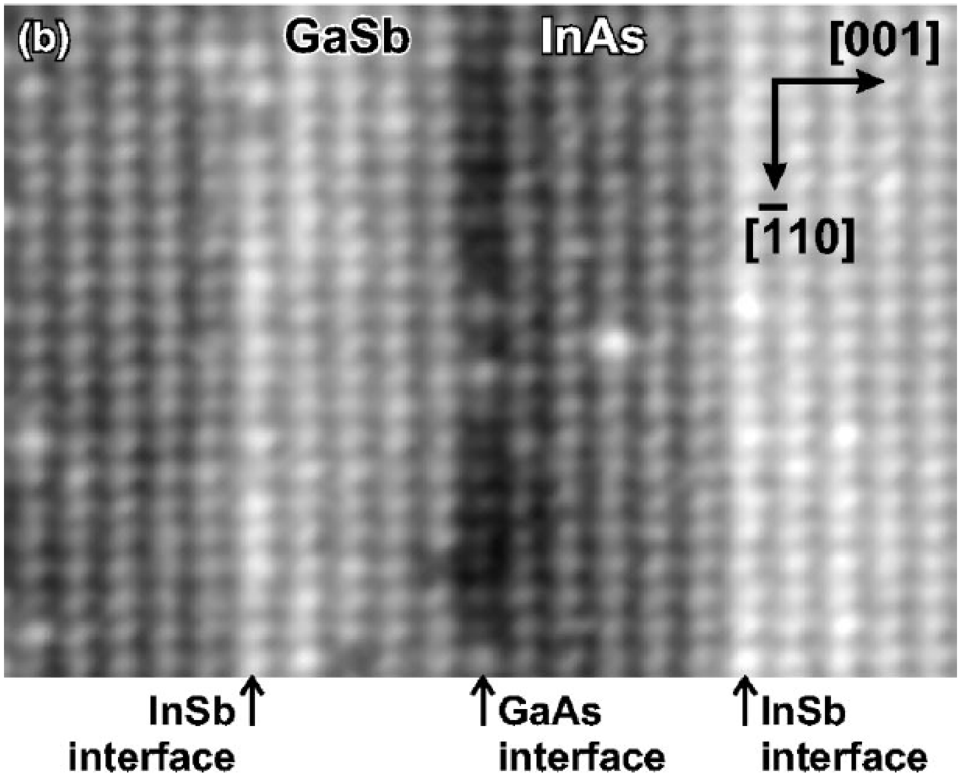

PHYSICAL REVIEW B 67, R121306 (2003)

(a) Relaxed geometry of a III-V (110) surface.

d_0: bond length in the bulk

d_1: surface III-V bond length indicated

d_2: III-V height difference at surface

(b) Constant-current, filled-state STM image of InAs/GaAs superlattice

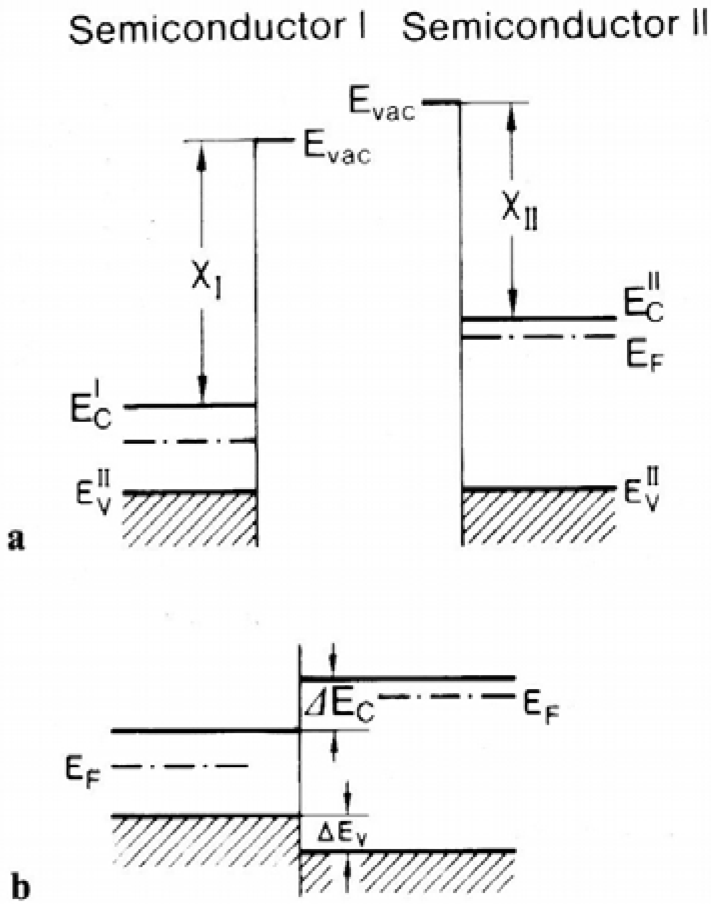

Im Gleichgewicht:

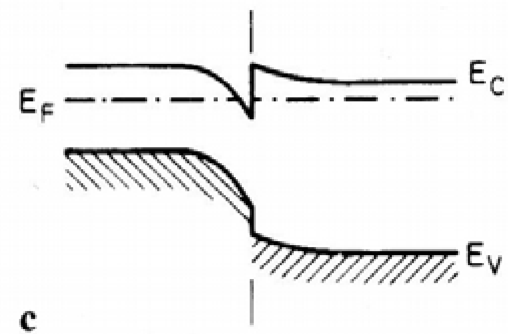

Fig. 12.22 a–c. Band schemes (one-electron energies plotted in real space) for a heterostructure formed from semiconductors I and II. **a** Semiconductors I and II are assumed to be isolated; χ_I and χ_{II} are the electron affinities, i.e., the energy between the vacuum energy E_{vac} and the lower conduction band edge E_C. **b** Semiconductors I and II are in contact, but not in thermal equilibrium because the Fermi levels E_F on the two sides have not equalized. ΔE_C and ΔE_V are the band discontinuities in the conduction and valence bands, respectively. **c** In thermal equilibrium, the Fermi energies E_F in I and II must be identical. Since the band discontinuities ΔE_C and ΔE_V are predetermined, band bending must occur in the two semiconductors

χ Elektronenaffinität

Leitungsbanddiskontinuität $\Delta E_C = \chi_1 - \chi_2$

(Obacht: Oberflächendipol, Defekt/Grenzflächenzustände)

Modulation doping

N-n heterojunction

I: wide gap heavily n-doped

II: narrower gap weakly n-doped

band scheme of superlattice

Verarmung Anreicherung

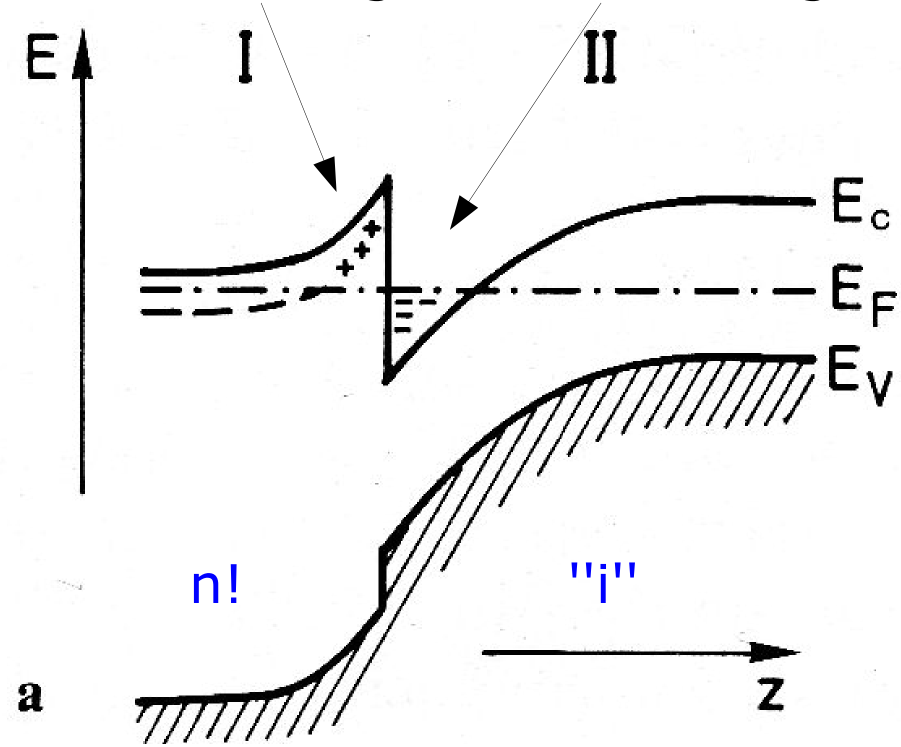

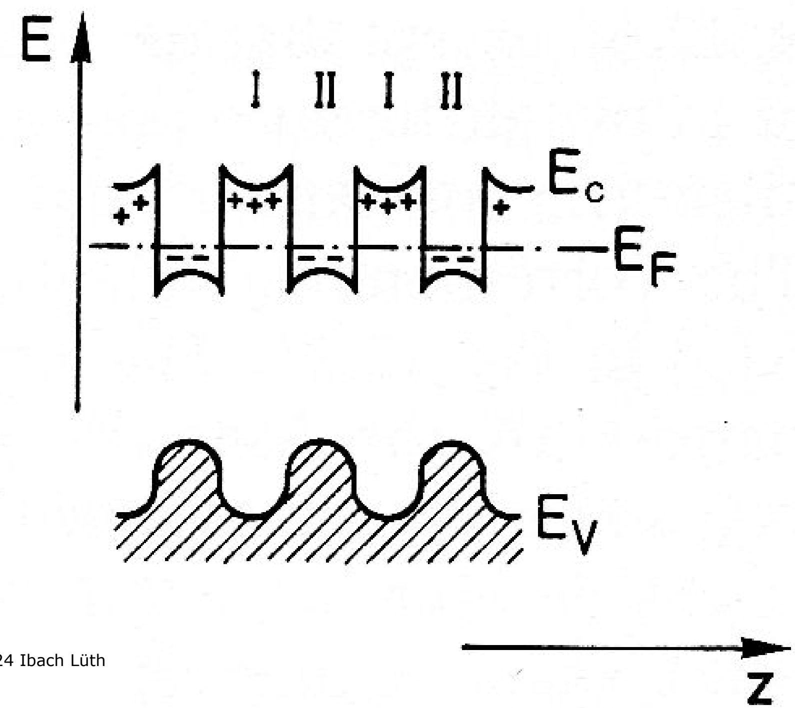

Fig. 12.24 Ibach Lüth

Electrons confined against AlGaAs
by E-field of dopants (Si^+)

Electron mobility of 2DEGs in modulation doped GaAs/AlGaAs

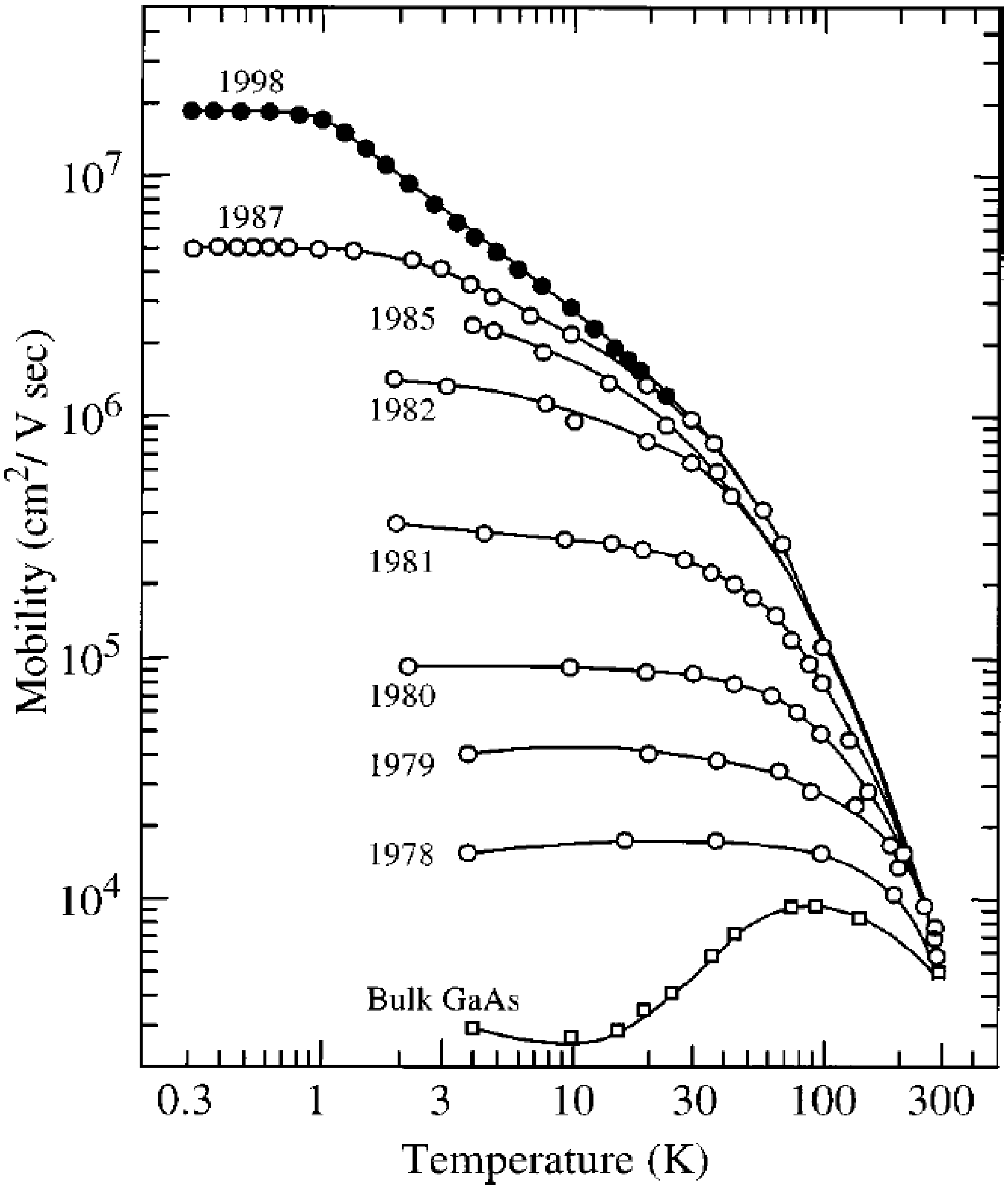

high T / lowest T: μ limited by scattering from phonons / defects

Progress made: Thousandfold increase of μ through modulation doping.

$\mu = 2 \times 10^7\ cm^2/Vs$ corresponds to 1/5 mm ballistic electron motion between collisions

Inventors of the modulation-doping processm, in 1978 around an early MBE machine at Bell Labs. From left: Willy Wiegmann, Art Gossard, Horst Störmer, Ray Dingle

Superlattices

Fig. 12.27. Energy states of electrons confined in the rectangular potential wells (inset) of the conduction bands of a composition superlattice; the potential wells have a width d_z which also corresponds to their distance from one another. For the calculation, an electronic effective mass of $m^* = 0.1\, m_0$ was assumed. The heavy lines in the shaded regions are the results for single potential wells with the corresponding widths d_z; potential wells in a superlattice with sufficiently small separation lead to overlap of wavefunctions and therefore to a broadening into bands (*shaded region*). (After [12.7])

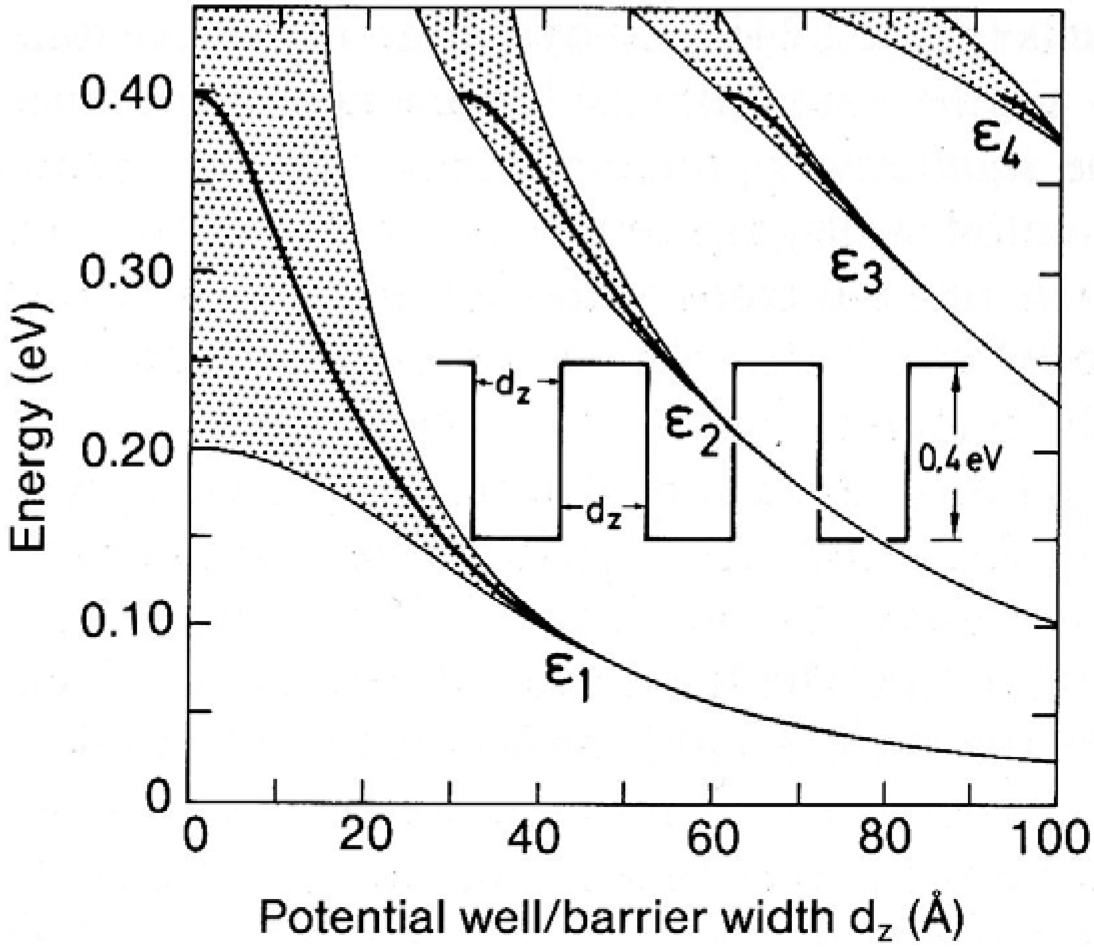

Light Absorption in Semiconductors

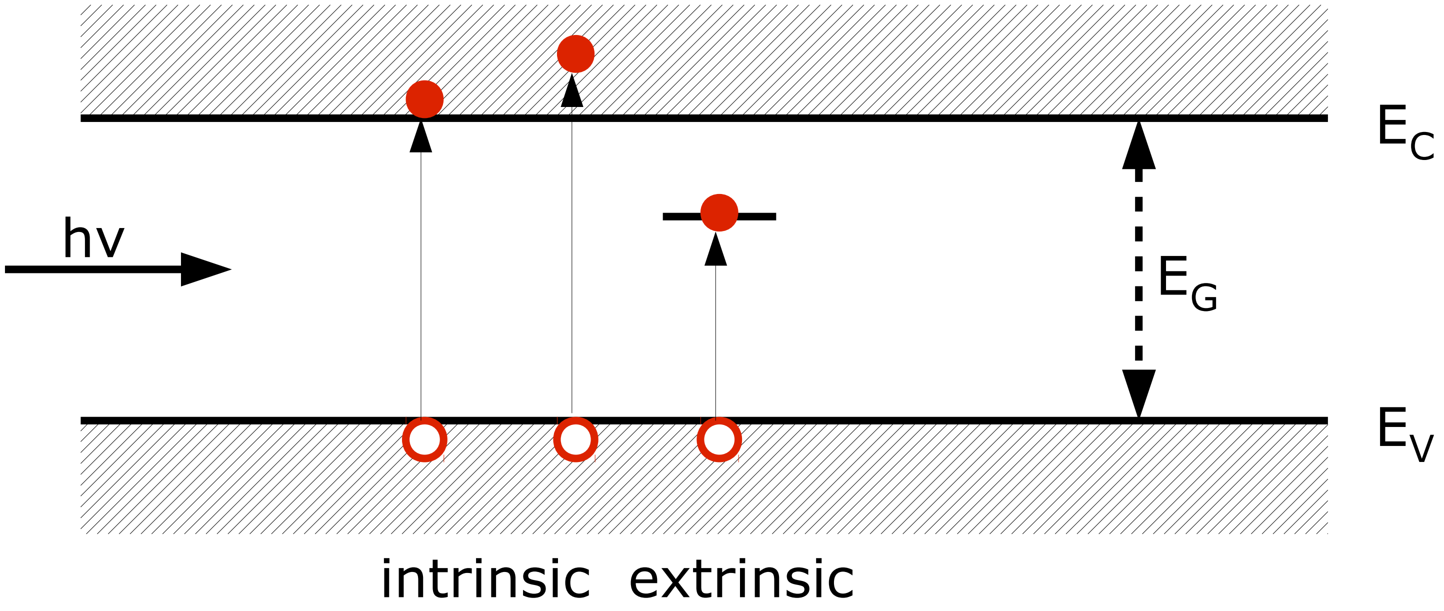

Luminescence

Photoluminescence

Cathodoluminescence; Minorityinjection, Impact Ionization

Excitons

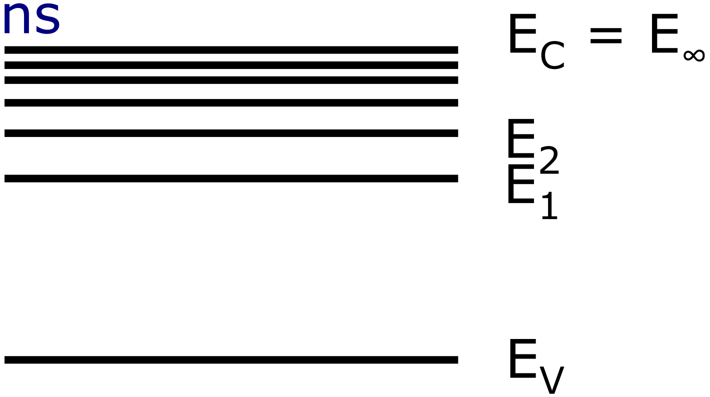

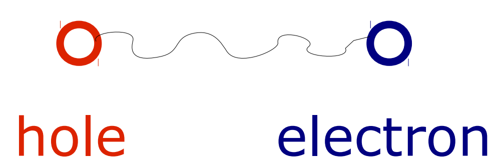

LED – Light Emitting Diode

diode at forward bias – recombination – radiation

GaAs	1.43 eV	870 nm	IR communication
GaP	2.26 eV	550 nm	green LED
$GaAs_xP_{1-x}$	variable		red LED
GaN	3.4 eV	405 nm	violet LED
$In_xGa_{1-x}N$	variable		blue LED

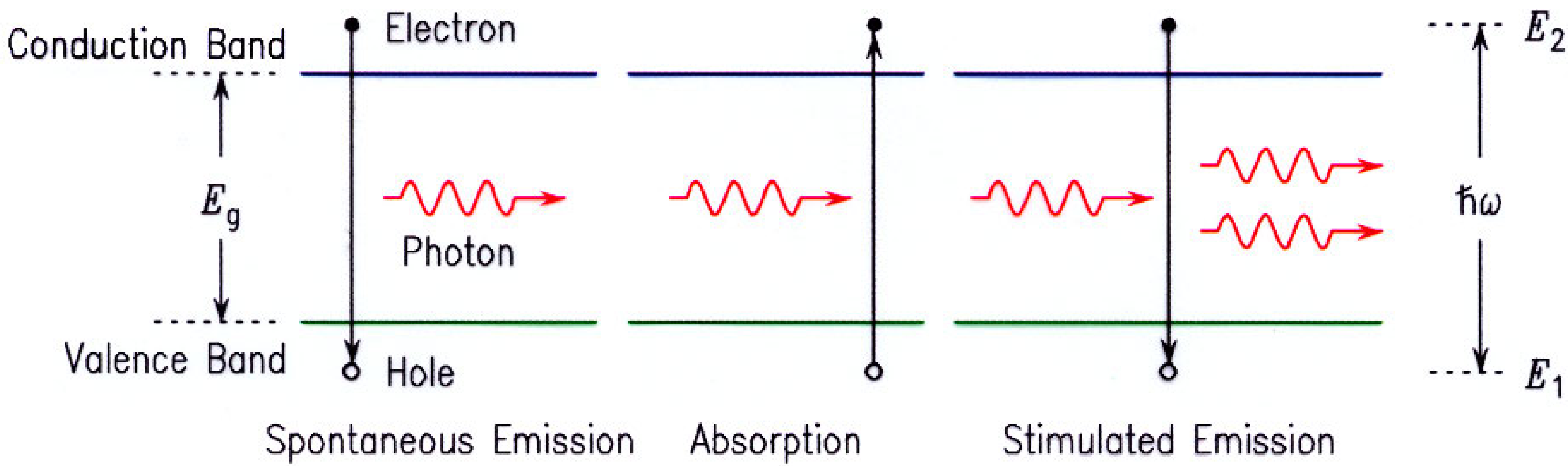

Conduction Band
Electron
E_g
Photon
Valence Band
Hole
E_2
$\hbar\omega$
E_1
Spontaneous Emission
Absorption
Stimulated Emission

Laser

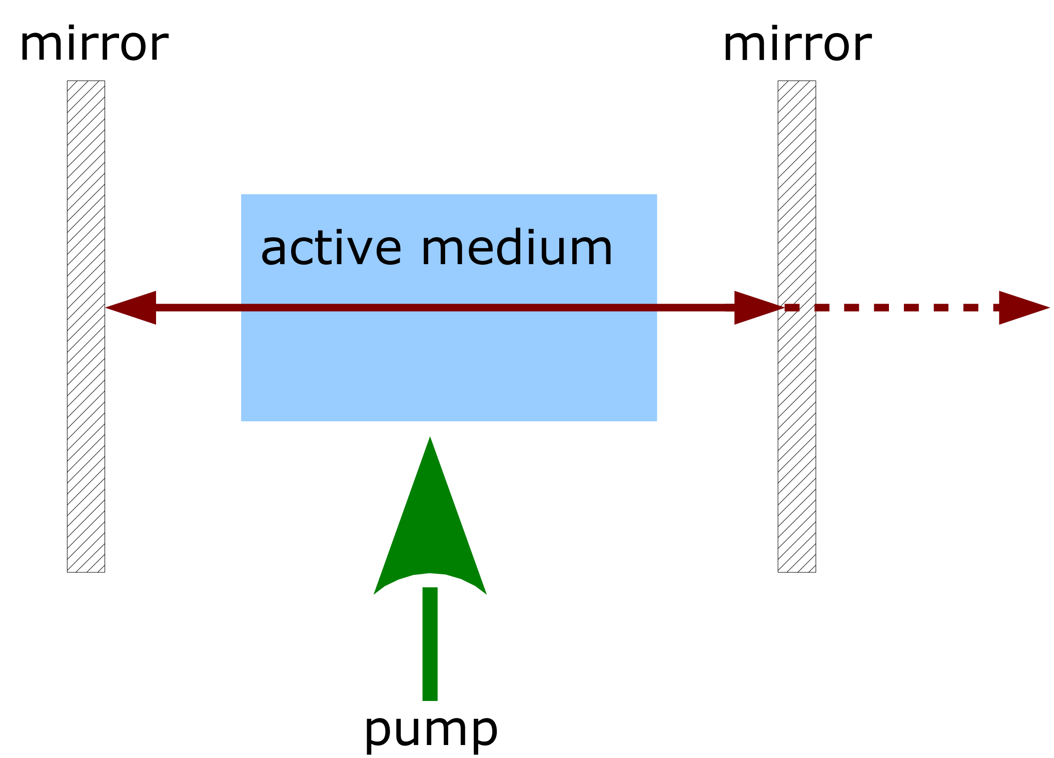

mirror
mirror
active medium
pump

Halbleiterlaser

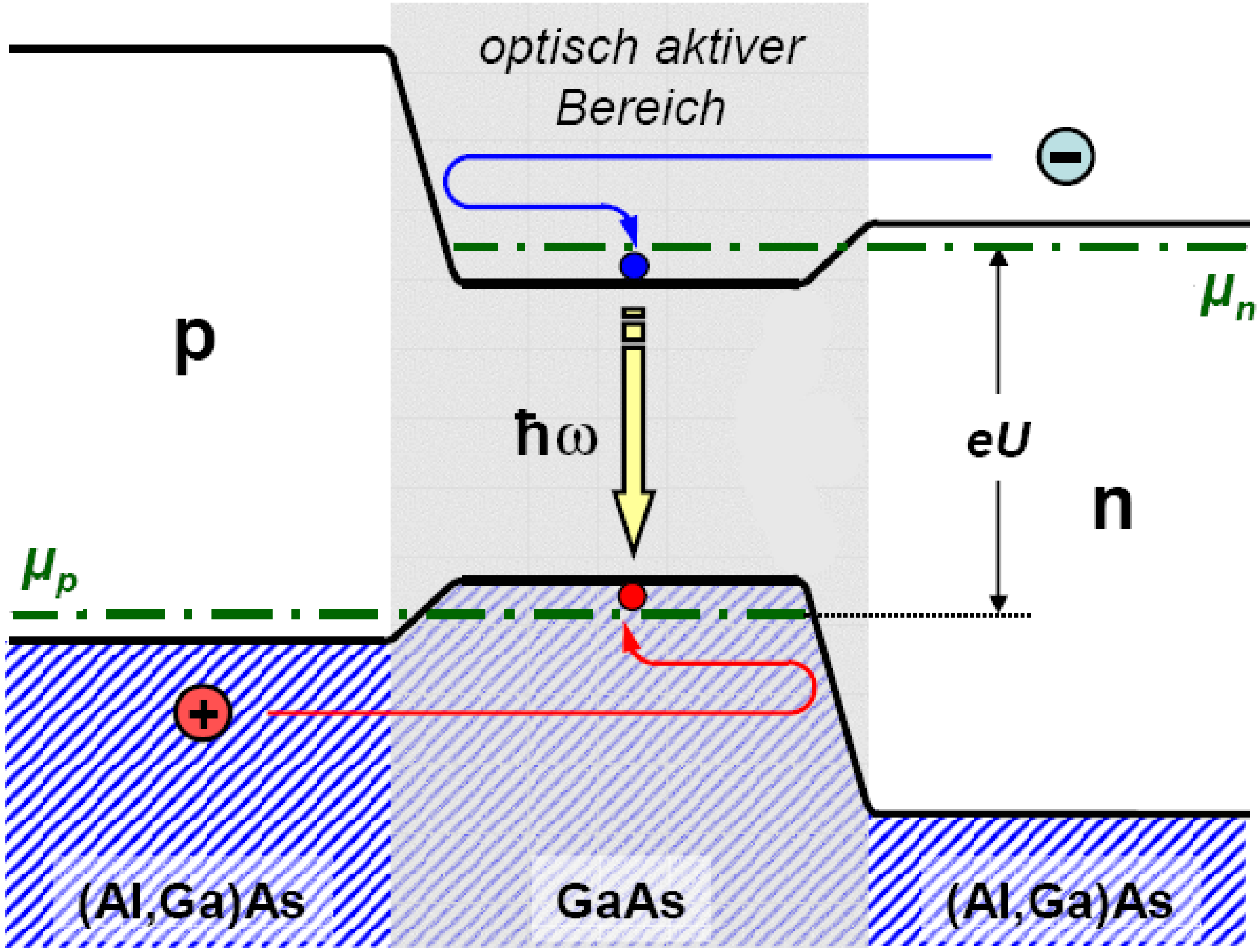

Halbleiterlaser

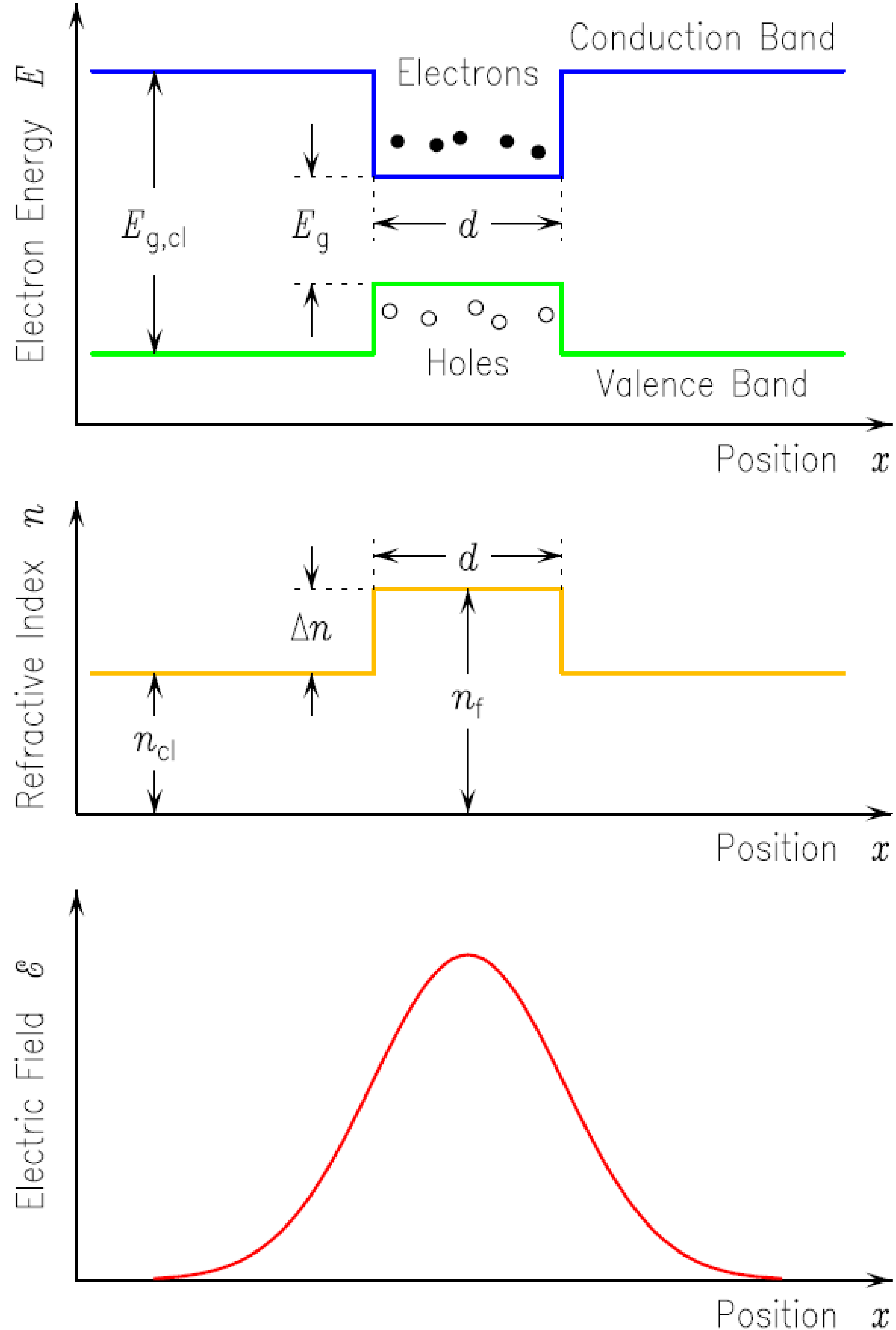

Resonator provides many standing wave modes

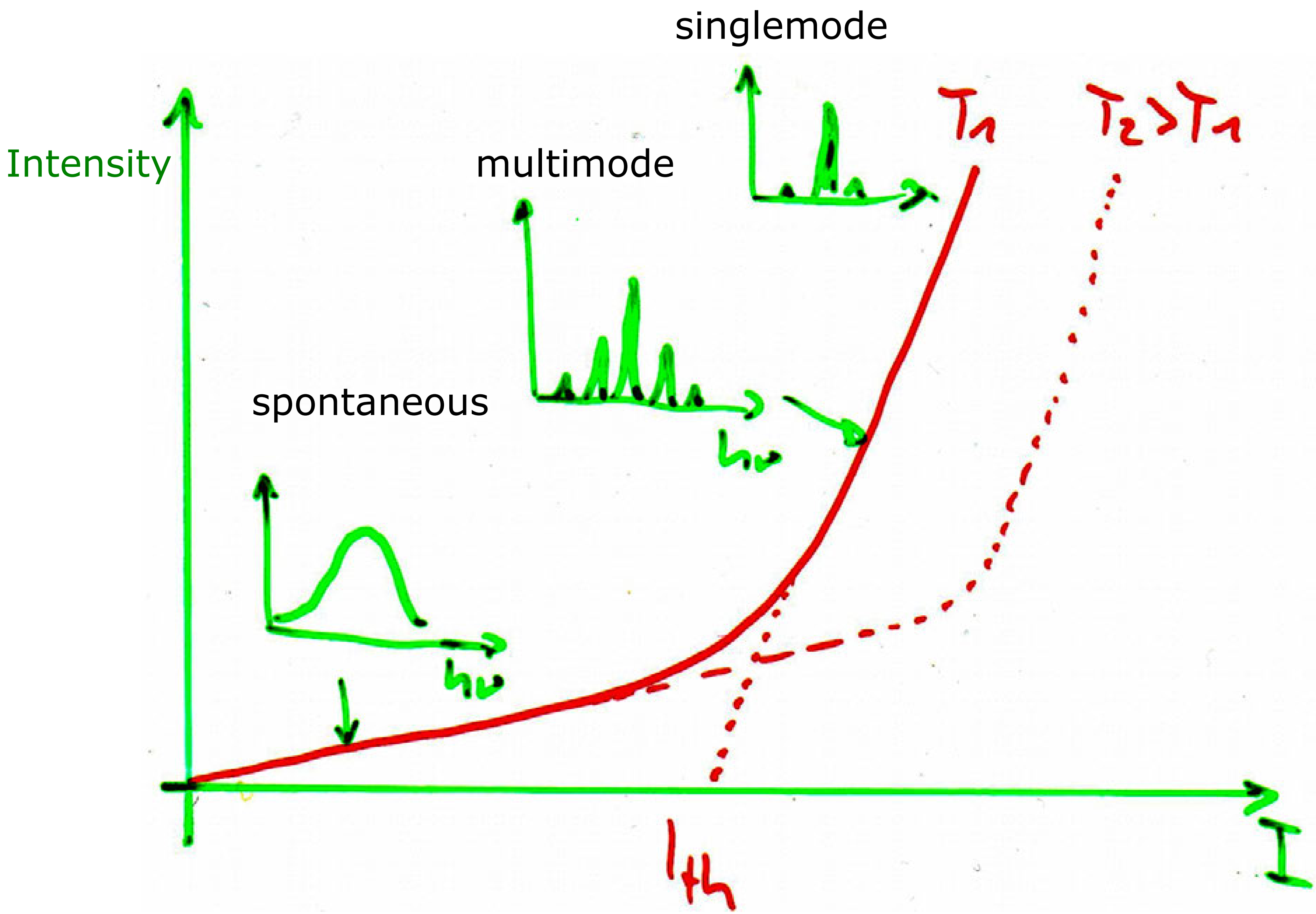

POPULARISING your science may lead to a terminal loss of serious reputation. So why not go for broke--as have the authors of "Britney's Guide to Semiconductor Physics"?

As you can read at http://britneyspears.ac/lasers.htm,

"It is a little known fact that Ms Spears is an expert in semiconductor physics. Not content with just singing, in the following pages, she will guide you in the fundamentals of the vital laser components that have made it possible to hear her super music in a digital format."

Halleffekt an 2D Elektronengasen

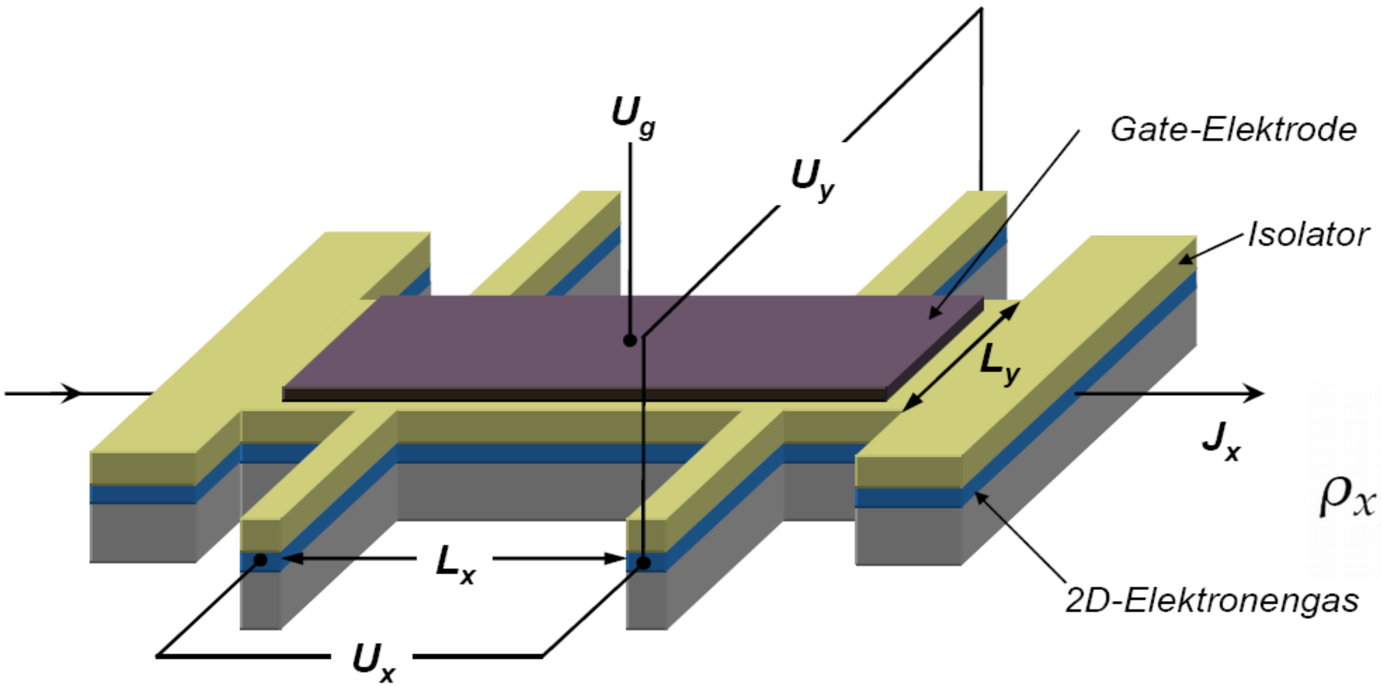

$$\rho_{xy} = \frac{B}{n_{2D} e} = R_H \cdot B$$

$$\begin{pmatrix} J_x \\ J_y \end{pmatrix} = \frac{\sigma_0}{1+\omega_c^2\tau^2} \begin{pmatrix} 1 & +\omega_c\tau \\ -\omega_c\tau & 1 \end{pmatrix} \begin{pmatrix} E_x \\ E_y \end{pmatrix}$$

$$\sigma_0 = \frac{n_{2D} e^2 \tau}{m^\star}$$

$$\omega_c = \frac{e\,B}{m^*}$$

$$\rho_{xx} = \frac{\sigma_{xx}}{\sigma_{xx}^2 + \sigma_{xy}^2} \qquad \rho_{xy} = \frac{-\sigma_{xy}}{\sigma_{xx}^2 + \sigma_{xy}^2}$$

$$\rho_{yy} = \rho_{xx} \qquad \rho_{yx} = -\rho_{xy} \; .$$

$$\sigma_{xx} = \frac{\rho_{xx}}{\rho_{xx}^2 + \rho_{xy}^2} \qquad \sigma_{xy} = \frac{-\rho_{xy}}{\rho_{xx}^2 + \rho_{xy}^2}$$

$$\sigma_{yy} = \sigma_{xx} \qquad \sigma_{yx} = -\sigma_{xy}$$

Ganzahliger Quanten-Hall-Effekt

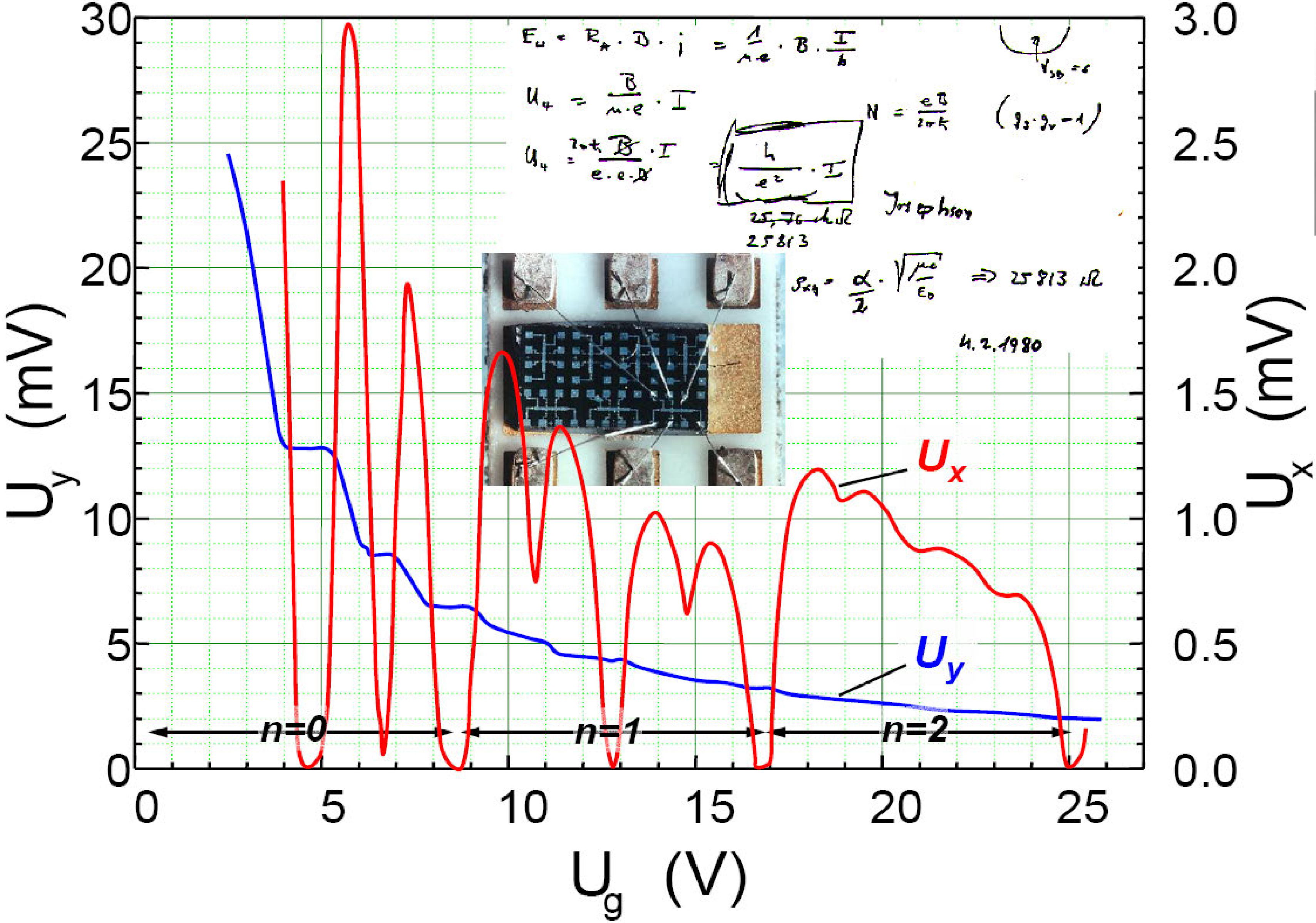

Nobelpreis 1985

$U_y = R_{xy} I_x$

K. von Klitzing,
G. Dorda,
M. Pepper,
Phys. Lett. **45**, 494 (1980)

2DEG in an external magnetic field

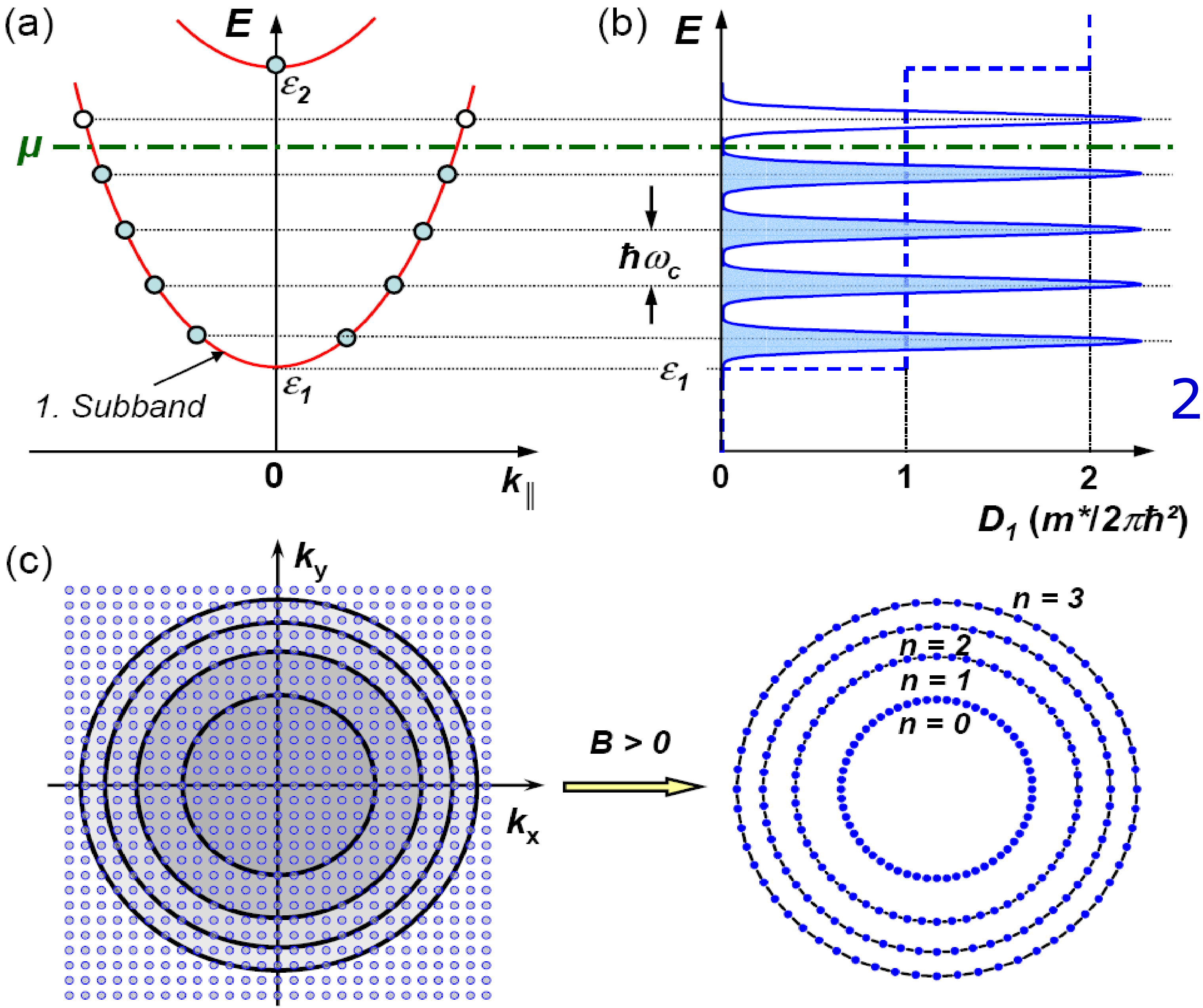

DOS:

2D box → peak

Entartung des untersten Landauniveaus

alle Spins parallel

n_l Zustände pro Fläche im Intervall $\hbar\omega_c$

$$n_l = \frac{g_l}{L^2} = \hbar\omega_c\, D(B=0) = \hbar\omega_c\,\frac{m^*}{2\pi\hbar^2} = \hbar\frac{eB}{m^*}\,\frac{m^*}{2\pi\hbar^2} = \frac{e}{h}B$$

$$R_H = \frac{B}{ne} = \frac{B}{i\,n_l e}$$

i Zahl der Landauniveaux

$$\rightarrow\ R_H = \frac{h}{e^2}\frac{1}{i} = \frac{1}{i}\,R_K$$

$$R_K = \frac{h}{e^2} = 25812{,}807572(95)\,\Omega$$

wenig später: Fraktionaler Quanten-Hall-Effekt

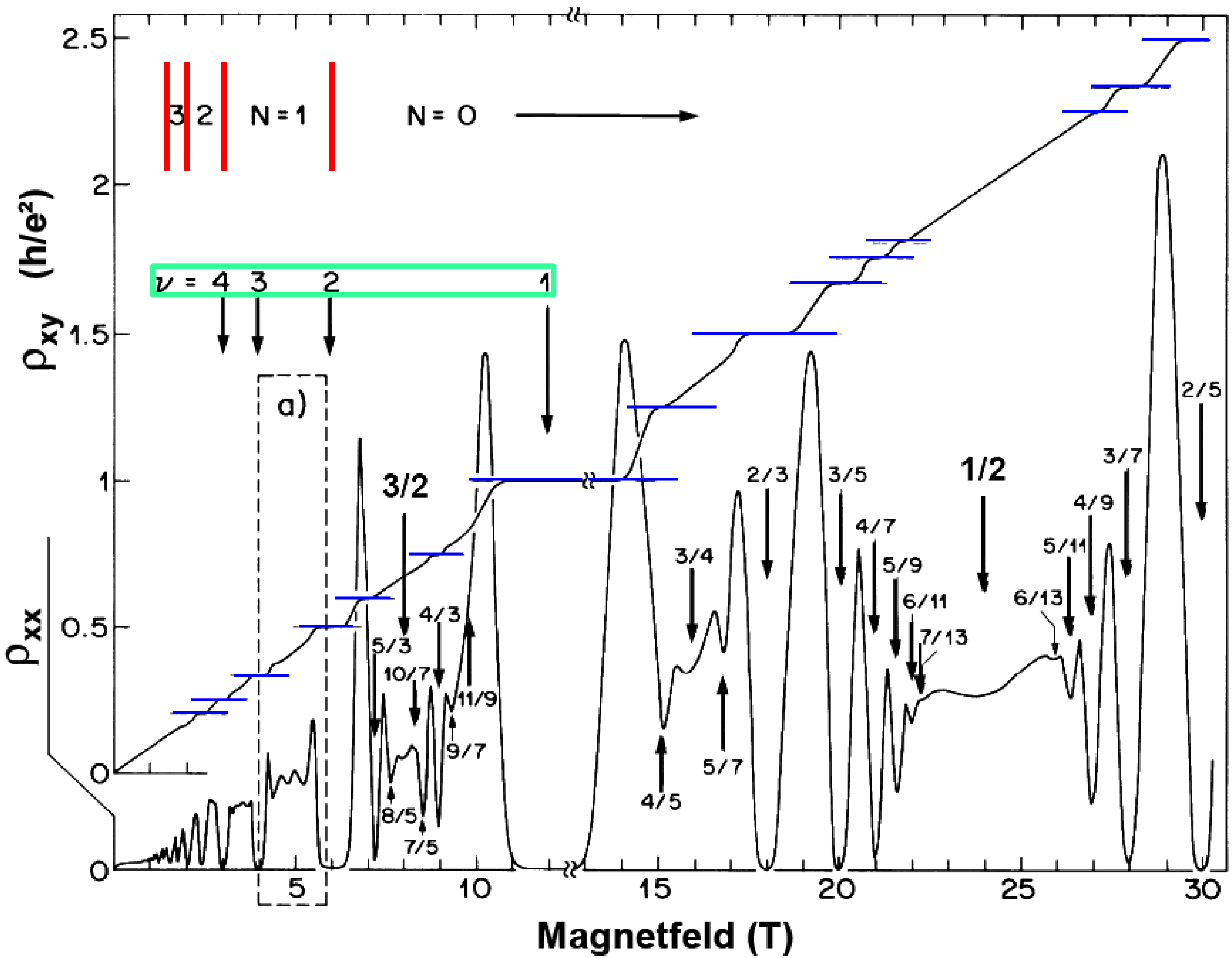

Nobel Lecture: The fractional quantum Hall effect

Horst L. Störmer, Rev. Mod. Phys. **71**, 875 (1999)

T. Kovacs, T. Duff, Bell Labs

Nobelpreis 1998

Störmer, Tsui, Laughlin

Linda A. Cicero /
Stanford News Service

Quantized conductance of point contacts in a 2DEG

B. J. van Wees et al., Phys. Rev. Lett. **60**, 848 (1988)

Ballistic point contacts, defined in the 2DEG of a GaAs-AlGaAs heterostructure

Conductance changes are quantized

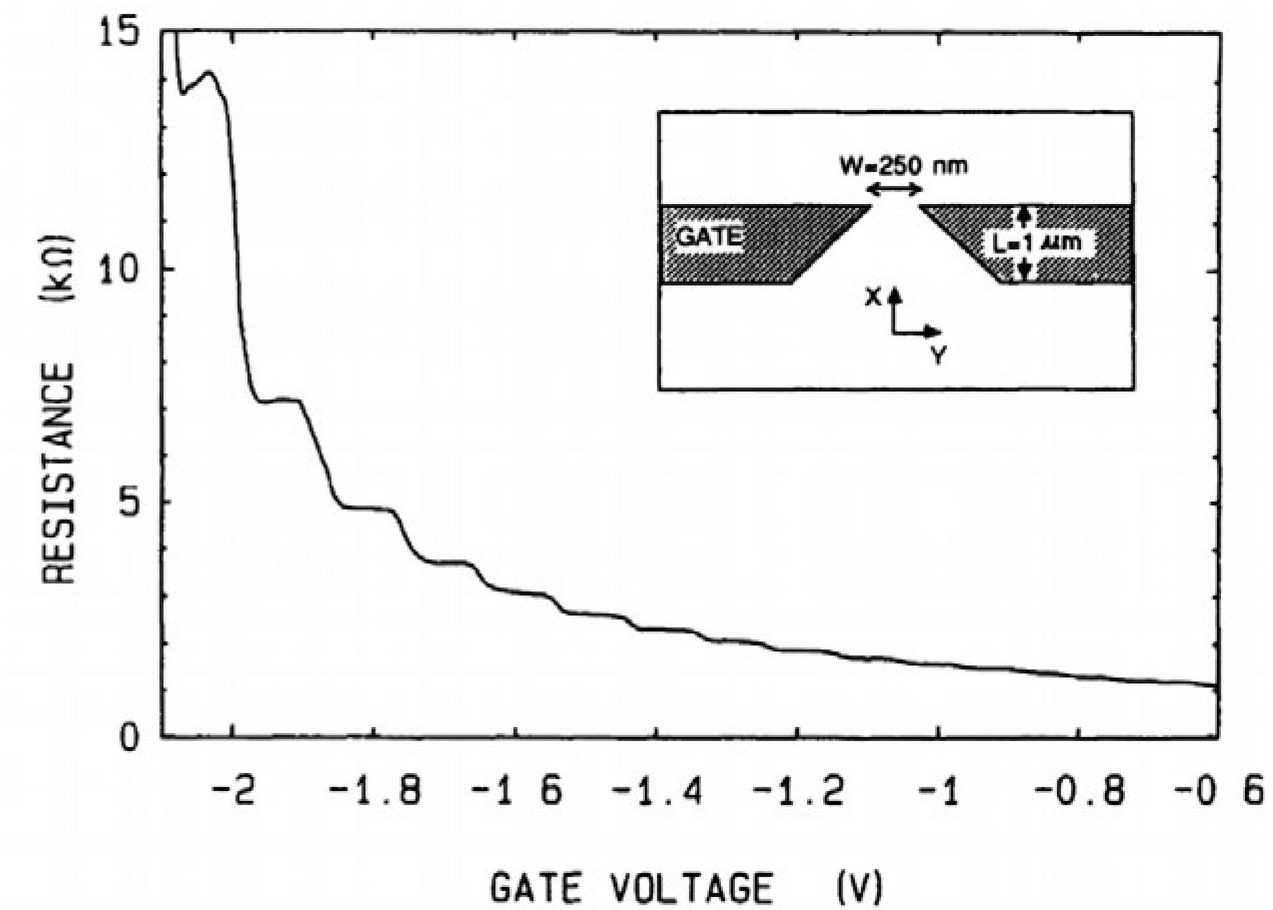

FIG. 1. Point-contact resistance as a function of gate voltage at 0.6 K. Inset: Point-contact layout.

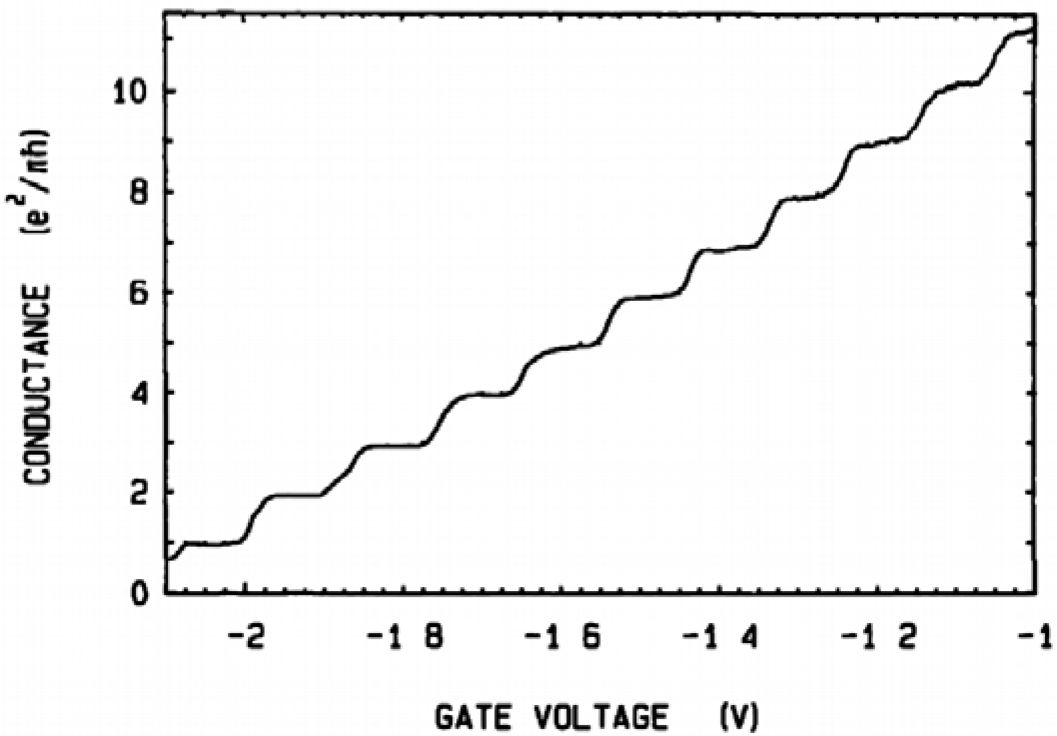

FIG. 2. Point-contact conductance as a function of gate voltage, obtained from the data of Fig. 1 after subtraction of the lead resistance. The conductance shows plateaus at multiples of $e^2/\pi\hbar$.

Landauerformel

$$G = \frac{e^2}{\pi\hbar} \sum_{n,m=1}^{N_c} |t_{nm}|^2$$

B. J. van Wees et al., Phys. Rev. Lett. **60**, 848 (1988)

Atomic-scale engineering of Cu electrodes

Schull, Frederiksen, Arnau, Sánchez-Portal, Berndt, Nature Nanotechnol. **6**, 23 (2011)

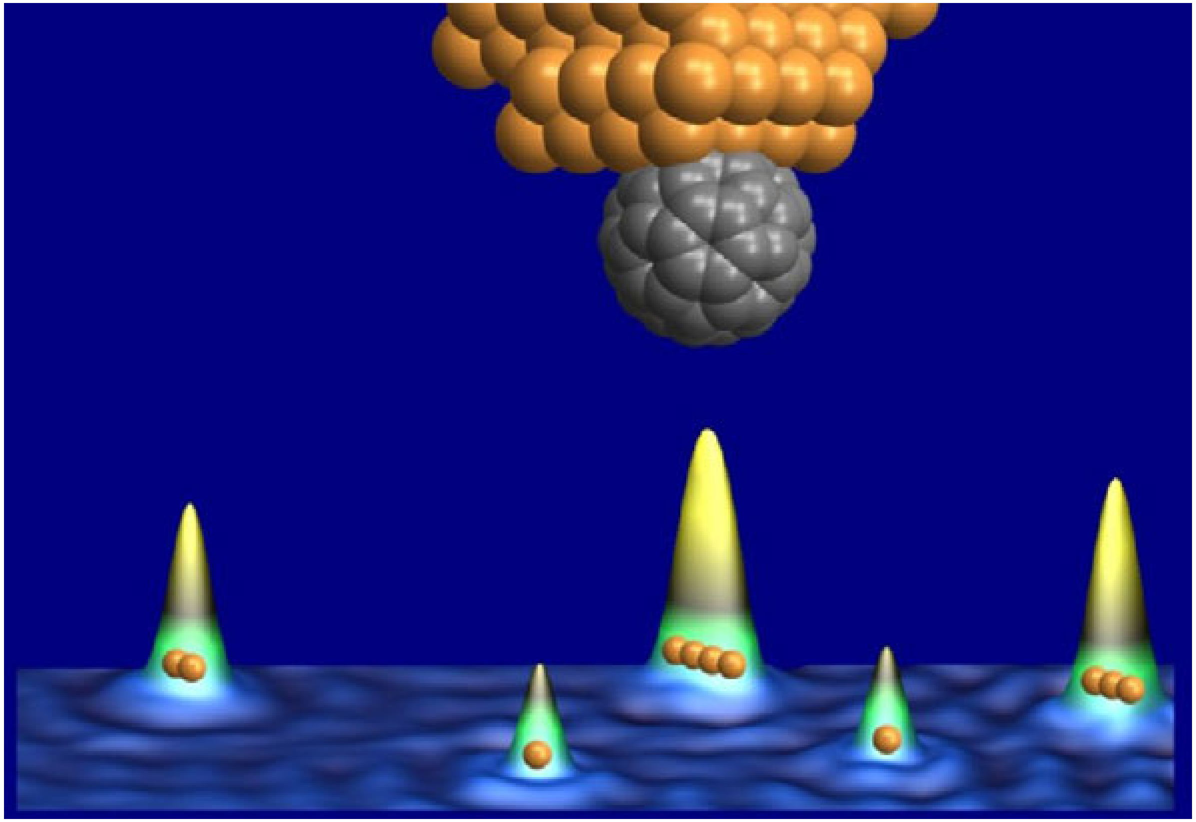

State-of-the-art

e-beam lithography

(hardly used)

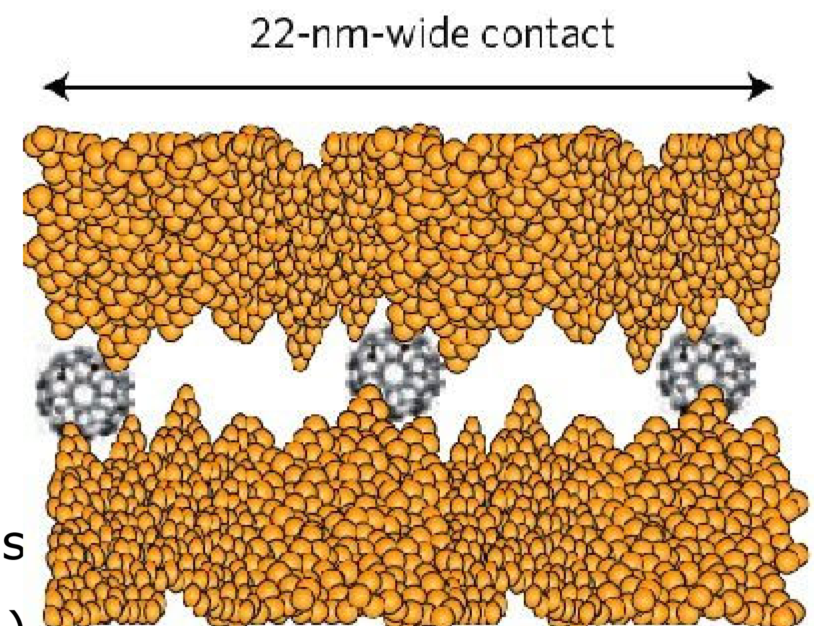

From A. Heinrich, Closing in on molecular junctions

Nature Nanotechnol. (news & views) **6**, 7 (2011)